8-2013

IMPACT OF CHANNEL CONDITIONS ON EXISTING SCOUR MEASURING INSTRUMENTS

Md nasimul hoque Chowdhury
Clemson University, chowdhury.nasimul@gmail.com

IMPACT OF CHANNEL CONDITIONS ON EXISTING SCOUR MEASURING INSTRUMENTS

A Dissertation
Presented to
the Graduate School of
Clemson University

In Partial Fulfillment
of the Requirements for the Degree
Master of Science
Civil Engineering

---

by
Md Nasimul Hoque Chowdhury
August 2013

Accepted by:
Dr. Abdul Khan, Committee Chair
Dr. Sez Atamturktur, Co-Chair
Dr. Nadarajah Ravichandran

ABSTRACT

Scour around bridge piers and abutments, is the prominent reason for bridge failures. Bridge failures have substantial effects on economy and human lives. About 60% of the total bridge failures in U.S. can be attributed to scour. In the past, scour has been responsible for several million dollars in bridge repair cost. Given the threat to the bridge infrastructure due to scour, the U.S. Federal Highway Administration has proposed several countermeasures to reduce the impact of bed degradation. One of these countermeasures that is particularly relevant during peak flow periods is the real-time scour monitoring. Scour monitoring involves real-time data collection to assess the progress of scour holes. Two of the most common scour monitoring systems are sonar/fathometers and time domain reflectometry.

This manuscript focuses on these two best in the class techniques to evaluate the effects of channel conditions on the accuracy of these systems. Through an extensive experimental campaign, the performance of these two monitoring techniques under different channel conditions, such as water temperature, salinity, and sediment concentration, is evaluated. The experimental results indicate that both time domain reflectometry and sonar methods are sensitive to the channel temperature and salinity. For a sonar device, such effects can be accounted for by modifying the speed of sound for different temperature and salinity levels. For the time domain reflectometry method, the temperature effects can be accounted for by using the same approach, while salinity degrades the waveform features limiting the device to non-saline environments. Furthermore, the time domain reflectometry is observed to be insensitive to suspended

sediment concentrations and turbid flow. Sonar, however, is found to be sensitive to the combined effects of moving turbid water. As the velocity of turbid water increases, the standard deviation in the sonar measurements increases. Eventually reaching a point at which the device can no longer yield an accurate reading of the bed. In addition to the impact of temperature, salinity, and suspended sediment, the sonar is also sensitive to additional operational conditions within the channel. Sonar is also tested in varying bed topography conditions to assess the impact of beam radius. The result reveals that the device records the minimum depth within the beam diameter.

In nature, channels flow under diverse conditions. So it is of great significance to evaluate which scour monitoring system is suitable under given conditions. Based on the results of experiments performed in this study, appropriate scour monitoring system can be chosen for a given channel conditions.

DEDICATION

To my beloved parents and my family for whom my whole life pertains.

ACKNOWLEDGMENTS

To enlist the entire number of persons to whom I am in debt for might not be possible, so in a few words I would like to say thank you to those who have made a mark on me and this project in particular.

Without the support and encouragement of my family, and in particular my parents Md Azimul Hoque Chowdhury and Ayesha Akhter Chowdhury, this work would not have been possible. I would also like to formally acknowledge the support, guidance, and direction that I have received from my committee chair, Dr. Abdul Khan. His insight and consultation has guided me through the challenges in this project. I would like to acknowledge my co-chair Dr. Sez Atamturktur for her support, guidance and time throughout my research and thesis. I would also like to acknowledge Dr. Nadarajah Ravichandran for the support and time in reviewing my thesis. I would like to convey my acknowledgment to my colleague Dr. Murray Fisher for giving support throughout my research work.

Lastly, I would like to conclude by acknowledging the support of the South Carolina Department of Transportation and Clemson University for their financial support during this project.

TABLE OF CONTENTS

Page

Table of Contents (Continued)

Page

LIST OF TABLES

Table Page

LIST OF FIGURES

Figure Page

List of Figures (Continued)

Figure Page

CHAPTER 1

INTRODUCTION

Bridge pier and abutment scour is ubiquitous. Bridges are considered an essential part in a transportation system. So, protecting the bridges from the events that can cause instability and ultimately failure has a great importance. Pier and abutment scour is the prominent reason behind bridge failures as mentioned in Lagasse et al. (1997), it accounts for 60% of the bridge failures. Bridge failures may be associated with direct loss of lives and an enormous repair cost. Thus, protecting bridges from scour has a great significance.

Local scour is the process by which bed materials around the piers and abutments of a bridge are continuously removed by natural flow. Damages due to scour can be reduced by armoring or replenishing bed materials or by regulating the peak flow so that the scour is restricted to a certain threshold. This threshold depends on the design consideration of the bridge in concern. Thus, scour monitoring that monitors scour depths around the bridge piers and abutments is essential. When the scour depth approaches the threshold, protective measures can be implemented.

There are generally three types of scours that affect the performance and safety of bridges, namely, local scour, contraction scour, and scour due to general aggradation and degradation of a channel reach (Parker et al. 1997). Local scour is the removal of sediment from around bridge piers and abutments. Water flowing past a pier and/or abutment may scoop out sediment forming a hole known as scour hole. Contraction scour is the removal of sediment from the bottom and sides of the river. It is caused by an

increase in the flow velocity as the water moves through a bridge opening that is narrower than the river upstream of the bridge. Scour arising from aggradation and degradation is due to long term removal/deposition of sediment in a river reach. The sediment removal and resulting lowering of the river bottom are a natural process, but may remove large amounts of sediment near bridge site over time (Deng and Cai, 2010). The total scour depth is determined by adding three scour components which includes the long-term aggradation and degradation of the river bed, contraction scour at the bridge, and local scour at the piers or abutments.

Following are the methods that have so far been used for the measurement of the scour depths (Fisher, 2012).

- Point scour measuring methods
  - Sounding rods
  - Float out devices
  - Magnetic sliding collar
  - Sonar/ Fathometer
  - Time domain reflectometry
  - Fiber optics
  - Temperature measurements
  - Piezoelectric film sensors
  - Mercury tip switches
- Distributive scour measurement
  - Radar

- Bridge vibration measurements
- Advanced sonar techniques

Of the methods mentioned above, sonar/fathometers and time domain reflectometry are the most commonly used methods. This manuscript focuses on these two methods to determine how the channel conditions such as temperature, salinity, turbidity may affect the accuracy in the measurement of scour depth. Chapter 2 explains the theoretical background behind the importance of considering these channel conditions. Chapter 3 gives the outline of the experimental setups that are used for the evaluation of the measurement devices. Chapter 4 and 5 discuss the experimental results on sonar and TDR, respectively. Finally, Chapter 6 summarizes the results of the study and indicates key channel conditions for scour measurement.

CHAPTER 2

LITERATURE REVIEW

2.1 Introduction

Scour damage to bridges, a widespread and costly threat to transportation infrastructure, can be countered with appropriate monitoring of the riverbed as pointed out in the U.S. Federal Highway Administration HEC-23. The available monitoring methods however, are sensitive to conditions in natural channels, such as temperature, turbidity, etc. Thus, understanding the impact of these conditions on the performance of existing scour monitoring methods is essential for the success of field deployments.

2.2 Background

Scour around bridge piers and abutments typically occurs during peak flow periods, such as floods or hurricanes, and has been directly linked to the failure of several bridges. During 1961-1974, of the 86 bridge failures that occurred, 46 were attributed to scour damage (Murillo, 1987). Flooding in the late 1980s and early 1990s in the Northeastern and Midwest U.S., respectively, resulted in damage to more than 2,500 bridges (Mueller, 2000). More recently, from 1996-2001, 68 bridge failures in the U.S. were attributed to scour (Lin et al., 2006). Overall, 60% of the failures of bridge structures are reported to be due to scour damage (Lagasse et al., 1997). Furthermore, approximately 21,000 bridges in the U.S. are scour critical (Hunt, 2009), while approximately 80,000 bridges are scour susceptible (Richardson and Price, 1993; Hunt, 2009).

Floods, often the main source of the increased flows, may cause extensive scour around piers and abutments of bridges and can cost millions of dollars in damage. Floods during the 1980s resulted in damages of $300 million, while in the 1990s individual floods caused as much as $178 million (Murillo, 1987; Butch, 1996). Brice and Blodgett (1978) reported that the repair cost for bridges is roughly $100 million per flood event. On an aggregate basis, the total annual budget devoted to scour repairs by the U.S. federal government (between Federal Emergency Management Agency and Federal Highway Administration projects) is $20 million annually (Rhodes and Trent, 1993). The costs illustrated above, however, only account for the impact to the infrastructure itself and neglect the additional costs to the afflicted population, who depend upon bridges as vital part of their transportation system. These additional costs have been estimated to be as much as five times the cost of the actual repairs (Rhodes and Trent, 1993).

While the financial costs can be significant, a bridge failure from scour may also cause loss of human life, which has occurred during the Schoharie Creek, Hatchie River, and Arroyo Pasajero River's bridge failures. In 1987, the I-90 bridge failed due to a scour hole that formed around a pier footing, resulting in the loss of 10 lives (N.T.S.B., 1987). The U.S. 51 bridge failure over the Hatchie River in Tennessee in 1989 was caused by the scour hole that formed due to migration of the main channel, which went undiagnosed (N.T.S.B., 1989) and resulted in the loss of eight lives. Seven lives were lost in 1995 in California when a 3 m deep scour hole formed on the I-5 bridge over the Arroyo Pasajero River (Arneson et al., 2012).

To counter these threats, 32 states have deployed scour monitoring systems. Sonic fathometer is one of the most prominent methods for monitoring scour with 104 fathometers installed on 48 bridges (Lagasse et al., 1997). The performance of these sonar based scour monitoring systems has been reported (Lagasse et al., 1997; Nassif et al., 2002; Hunt, 2005; Mason and Sheppard, 1994; DeFalco and Mele, 2002; Holnbeck and McCarthy, 2011; Cooper et al., 2000). These reports have documented accurate measurements of scour hole depths, ranging from 0.23 to 1.2 m, as well as successful operation during hurricanes. While sonar systems have been used extensively, conditions in rivers can impact the performance of the device. These conditions include air bubbles entrained in the flow, suspended sediment and turbidity, debris, salinity, and temperature. DeFalco and Mele (2002) attributed the cause of 5 m spikes in the measured time histories of two bridges in Italy to the presence of air bubbles and suspended sediment/turbidity in the channel flows. Lagasse et al. (1997) reported the inability of sonar devices to determine the bed depth in conditions with significant air entrainment. Additionally, factors that affect the speed of sound, such as temperature and salinity, accounted for a 0.5 m offset in testing on a bridge over an inlet in Florida (Lagasse et al., 1997). Another factor that can have a significant impact on the performance of a sonar system is the presence of debris in the channel. Debris can result in false echoes, leading to inaccurate readings, or direct failure of the device as it physically impact the hardware or cabling. Cooper et al. (2000) reported that debris damage led to the loss of the entire hardware system in field tests in Indiana. Lastly, sonar pulses are emitted as a discrete cone defined by the hardware itself. As the pulse reaches the scour hole, its diameter may

be smaller or larger than the hole itself, depending upon the distance between the sonar and riverbed. In this case, if the hole is small relative to the beam diameter at the bed, it is possible to have reflected waves returned by the unscoured channel bed, which presents a problem for the determination of scour with sonar devices.

Another scour monitoring technique that has received attention is time domain reflectometry (TDR), which uses electromagnetic (EM) waves to determine the location of water/sediment interface. The TDR system consists of rods buried into the riverbed that act as waveguides for EM pulses. The EM pulses are reflected at various interfaces, such as the water/sediment interface or the air/water interface. TDR devices have been studied extensively in the lab and the investigations have included evaluating the device precision with various sediments, the impact of suspended sediments in the water as well as salinity effects (Yankielun and Zabilansky, 1999; Yu and Yu, 2006; Yu and Yu, 2011; Yu and Zabilansky, 2006). The TDR device has also been used to monitor the development of scour under ice at the Hwy 16 Bridge in Missouri, where the growth and refill of scour holes on the order of 0.15 m were measured (Ettema and Zabilansky, 2004; Zabilansky and Ettema, 2002). While the method is more robust than sonar to debris, sensitivities of the TDR device to conditions within the channel remain a concern. The effect of salinity levels, which can vary from 0.50 PPT (Parts per thousands) in the upper reaches of a watershed to 17.5 PPT in near coastal waters (USGS, 2006a; USGS, 2006b), on the performance of TDR measurements is not previously studied. Similarly, the water temperature, which can vary from 7 to 20 °C (USGS, 2006a; USGS, 2006b),

can affect the speed of the EM pulse and lead to inaccuracies in the measured TDR lengths.

To study the variability in the measured scour depth due to channel conditions, an experimental campaign is undertaken to evaluate the performance of sonar fathometer and TDR instrument under simulated field conditions. The performance of the sonar and TDR are considered under the following channel conditions, where appropriate:

- Saline conditions, from 0 to 35.5 PPT;
- Water temperatures, from 5 to 40 °C;
- Water with suspended sediments, for turbidities up to 900 NTU, including stratification effects;
- Scour hole size.

2.3 Sonar

Sonar as scour measuring system consists of two components. One is the transducer and the other is for data collection. Transducer engages piezoelectric crystals that are either connected to a membrane or diaphragm. When an electric potential is applied across the crystal, an electric field is induced, which causes strain and thus, displacement of the crystal and the membrane. This field is then cycled, yielding an acoustic wave that travels through the surrounding fluid (Jaffe and Berlincourt, 1965; Guo et al., 1992). As the acoustic wave propagates into the water in the channel, surfaces and objects will reflect part of the signal back which is called echo signal. Time elapsed between the emitted signal and reflected signal indicates the position of the object or surface from which the signal is reflected. A typical installation is illustrated in

Figure 2.1. A parameter that is fundamental to the operation of the sonar transducer is the speed of sound in water, c as shown in Equation (2.1), where D is the distance from the sonar transducer to the scour hole and t_{ECHO} is the echo time.

$$D = \frac{c \cdot t_{ECHO}}{2} \tag{2.1}$$

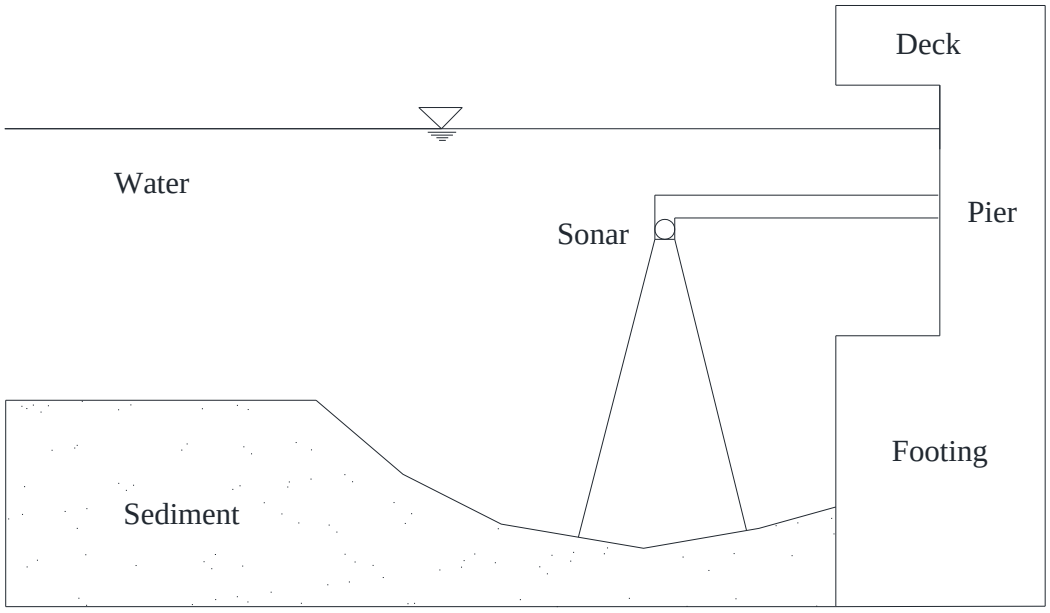

Figure 2.1: Typical installation of Sonar (Based on Nassif et al., 2002 ; Fisher 2012)

2.4 TDR

Time domain reflectometry based scour measuring system consists of a TDR device which emits high voltage pulse through a coaxial cable which is connected to a probe known as scour probe. The pulse propagates into the transmission line, which is a function of the speed of light, the electrical and physical characteristics of the

transmission line, and the surrounding media. The pulse propagates down the transmission line until the end of the line or some intermediate discontinuity is reached, where it is reflected back towards the source. The time t (in seconds) that it takes for the pulse to propagate down and back the length of the transmission line (L) is called the ‘‘round trip travel time’’ (Yankielun and Zabilansky, 1999), and is given by Equation (2.2) .

$$t = \frac{2L}{v} \tag{2.2}$$

Where v is the propagation velocity of the pulse, which can be calculated by Equation (2.3) .

$$v = \frac{c}{\sqrt{K}} \tag{2.3}$$

Where c is the speed of light and K is the relative dielectric constant of the media surrounding the transmission line (Yankielun and Zabilansky, 1999).

As the EM pulse propagates through the transmission line it may encounter different kinds of boundaries, such as air-water interface and water-sediment interface. When such boundaries are encountered, a portion of the emitted pulse energy is reflected back to the source and the rest continues to move further until another such boundary is encountered. This process continues till all of the emitted pulse energy is reflected back. Measuring the travel time of the pulse and knowing the dielectric constant of the medium through which the pulse is traveling permits calculation of the physical distance from the TDR source to each of the boundary encountered (Yankielun and Zabilansky, 1999).

A typical TDR signal is shown in Figure 2.2. Where point ‘A’ indicates the start of the probe, point ‘B’ indicates the reflection from the sediment/water interface and point ‘C’ represents the end of the probe. Apparent length can be interpreted from the TDR waveform signal which assumes the EM pulse speed as the speed of the light. From the apparent length, the actual physical length can be calculated from dividing the apparent length by square root of dielectric constant of the medium in consideration. If the distance travelled in sediment is $L_{a,s}$ and the distance travelled in water is $L_{a,w}$ in terms of apparent length, than the actual physical length can be calculated by Equations (2.4) and (2.5) where $K_{a,w}$ and $K_{a,s}$ are the apparent dielectric constant of water and sediment respectively. L_s and L_w represent the actual physical distance in sediment and water (Yankielun and Zabilansky, 1999).

$$L_s = \frac{L_{a,s}}{\sqrt{K_{a,s}}} \tag{2.4}$$

$$L_w = \frac{L_{a,w}}{\sqrt{K_{a,w}}} \tag{2.5}$$

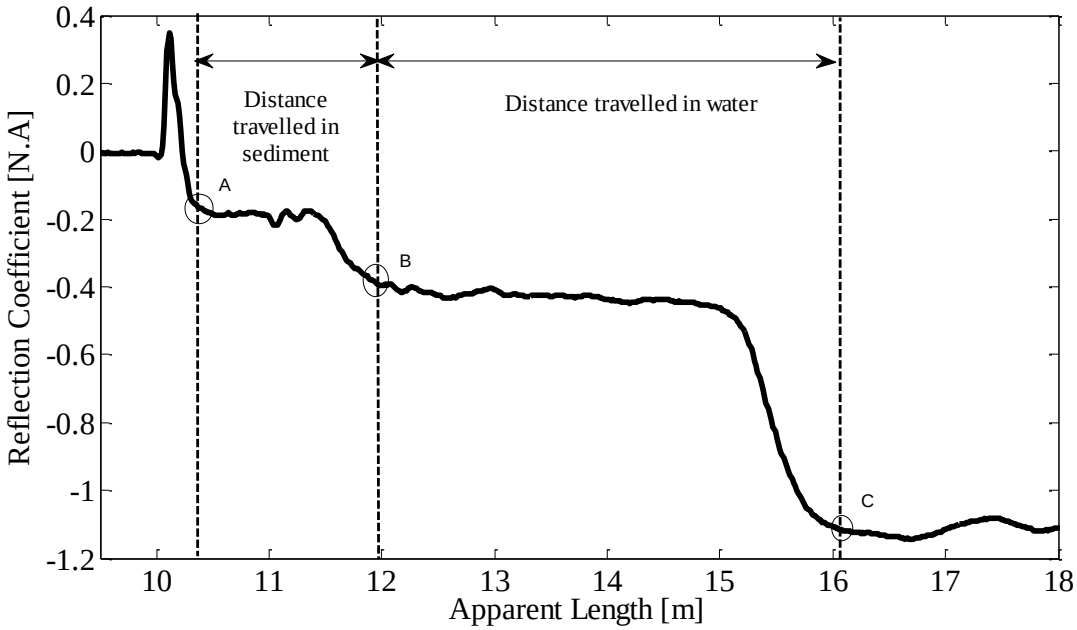

Figure 2.2: Typical TDR waveform

2.5 Studies of Factors Affecting Sonar

The speed of the acoustic pulse, given in Equation (2.1), is assumed to be constant. However, it has been shown to vary with temperature, salinity and depth (Kuwahara, 1939; Leroy, 1969; Urick, 1975; Mackenzie, 1981). For a typical temperature variation from summer to winter of 30 to 10 °C, corresponding errors in a sonar measurement due to changes in the speed of sound are shown in Figure 2.3. The three curves correspond to the equations for the speed of sound, as presented by Mackenzie (1981), Kuwahara (1939), and Leroy (1969) which are given by Equations (2.6), (2.7), and (2.8), respectively. In these equations, c is the speed of sound in m/s, T is the temperature in degrees Celsius, S is the salinity in PPT, and D is the depth in meters. For a temperature change of 20 °C, a sonar transducer can have an error up to 4% in the

distance to the riverbed. In turn, that 4% would correspond to nearly 0.15 m for an initial depth of 3.75 m. This is several times larger than the typical resolution of the device (about 3 cm) and thus, cannot be ignored.

$$\begin{aligned} c = {} & 1448.96 + 4.591T - 5.304\times10^{-2}T^2 + 2.374\times10^{-4}T^3 + \\ & 1.340\left(S-35\right) + 1.630\times10^{-2}D + 1.675\times10^{-7}D^2 - \\ & 1.025\times10^{-2}T\left(S-35\right) - 7.139\times10^{-13}TD^3 \end{aligned} \tag{2.6}$$

$$c = 1445 + 4.664T - 0.0554T^2 + 1.307\times\left(S-35\right) + 0.01815D \tag{2.7}$$

$$\begin{aligned} c = {} & 1492.9 + 3\left(T-10\right) - 6\times10^{-3}\left(T-10\right)^2 - 4\times10^{-2}\left(T-18\right)^2 + \\ & 1.2\left(1000S-35\right) - 10^{-2}\left(T-18\right)\left(1000S-35\right) + D/61 \end{aligned} \tag{2.8}$$

Similarly, the changes in the speed of sound due to salinity must also be considered. Variations occur in coastal waterways subject to tides or for inland waters during rainfall events, where the runoff could contain chemicals and other pollutants that would change the apparent salinity. The impact on the sonar due to changes in the salinity of the channel flow can also be evaluated by Equations (2.6), (2.7), and (2.8). Figure 2.4 reveals an increase in the uncertainty of approximately 2% in the scour measurements due to salinity effect.

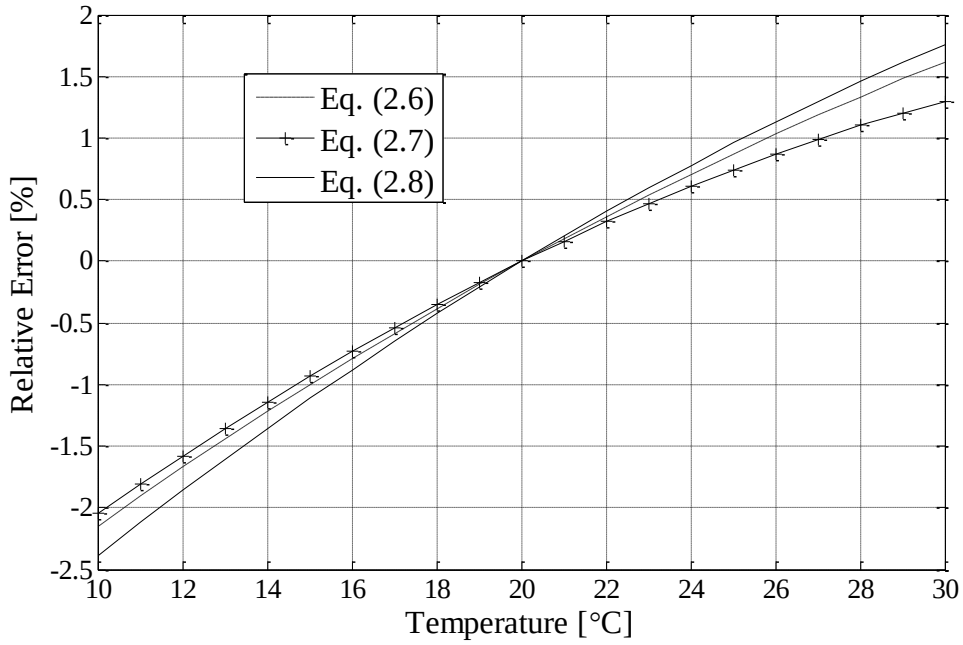

Figure 2.3: Relative error in distance measurements due to temperature changes, relative to the value at 20 °C ($c = 1500\ m/s$).

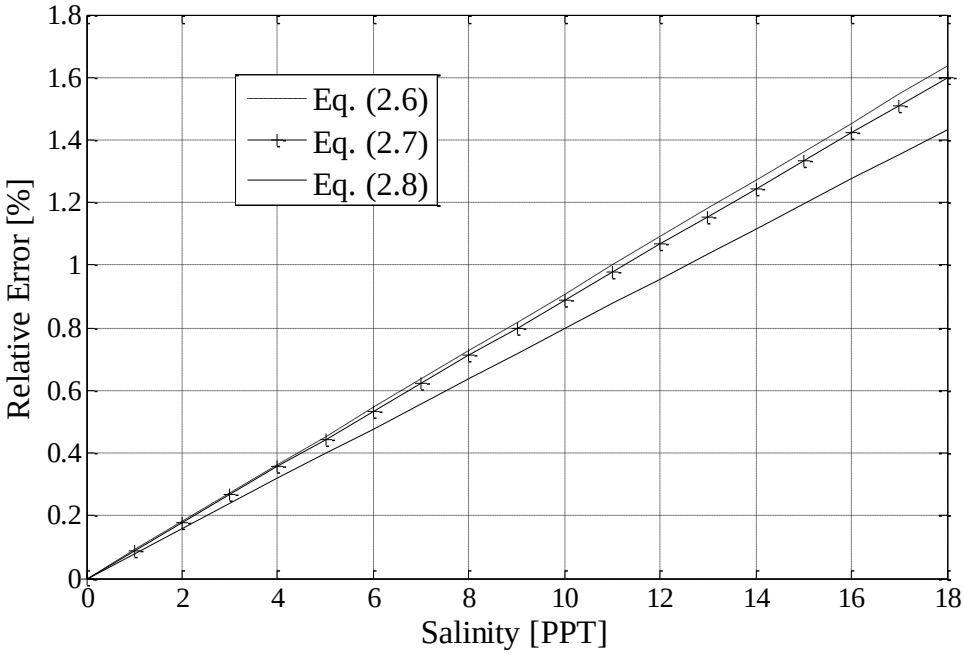

Figure 2.4: Relative error in distance measurements due salinity, relative to the speed of sound at 20 °C and 0 PPT.

In addition to being affected by the temperature and salinity of the water, the ability to make accurate measurements can depend upon the nature of the bed itself. Natural riverbeds typically have a defined transition between the water, ρ_0 and bed densities, ρ_2 , with an intermediary density between that of the sediment and the channel flow, ρ_1. This transition is typically defined by an initial step change from the water density to the near surface sediment density followed by a gradual transition to the final deep bed density (Hamilton, 1980), as shown in Figure 2.5. Robins (1990) presented a model for the propagation of sound waves in a fluid of varying density and developed a generalized model for the response of the sound wave as it encounters a density gradient. The reflection coefficient, defined as the ratio of the reflected to incident signals at an interface, can be affected by the stratification of sediments along the sonar pulse. For the general case described above, the result is a complex function of vertical wave number, k_z , which is the ratio of signal frequency to speed of sound. The reflection coefficient, as shown in Equation (2.9), is a function of the lower-bed density, the water density, the intermediate zone density, the density gradient thickness, h, and k_z. Robins (1990) showed that as the product $k_z h$ approaches zero and infinity, the reflection coefficient approaches values as shown in Equation (2.9).

$$\begin{aligned} \underset{k_z h \to 0}{R} &\to \frac{\rho_2 - \rho_0}{\rho_2 + \rho_0} \\ \underset{k_z h \to \infty}{R} &\to \frac{\rho_1 - \rho_0}{\rho_1 + \rho_0} \end{aligned} \tag{2.9}$$

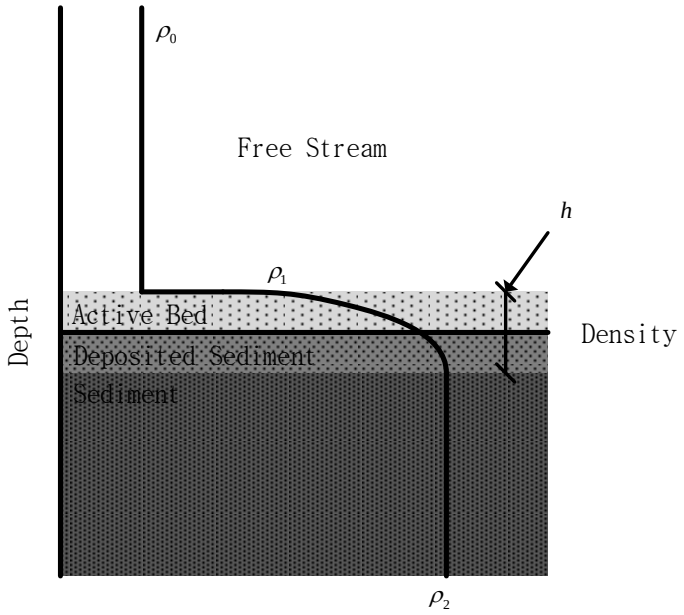

Figure 2.5: Density variation from the channel flow through the riverbed bottom, adapted from Robins (1990).

The implication of the results shown in Equation (2.9) is that at lower $k_z h$, and in turn at lower frequencies, the reflected signal is only a function of the density difference between the final bed density and the flow density and is independent of the intermediate value. Conversely, as the frequency increases the results of Robins predicts that the reflection coefficient reflects only from the initial step change between the channel and the riverbed. Stoll and Kan (1981) developed a more complex model that accounts for the effects of a porous, viscoelastic, saturated sediment and included the losses associated with the propagation of sound waves in the sediment structure and the saturated pores. The model includes the effects of porosity, grain size, permeability of the sediment, and internal stresses; and predicts the reflection coefficient as a function of the incidence angle and acoustic signal frequency. Stoll and Kan's (1981) results for incidence angles

less than 45 to 50° are relatively insensitive to frequency and collapsed to the Robins'(1990) results for low vertical wave number. Above 50°, the model predicts a reflection coefficient that is a function of frequency and rapidly approaches a value of 1.0. The Stoll and Kan's (1981) model for varying incidence is useful for scenarios where the sonar waves are not perpendicularly incident on the riverbed. However, for the typical configurations seen in river scour monitoring the model from Robins (1990) will suffice.

To explore Robins' model, the reflection coefficient is plotted in Figure 2.6 (a, b) as a function of the riverbed density and the intermediary material density, respectively. Figure 2.6 reveals that for various bed densities, the reflection coefficient varies in the range of approximately 0.2 to 0.3. For the suspended sediment to approach these values, the concentration has to reach 800 g/L. This value is well above the 10 g/L typically found in channels (Gray et al., 2003). Thus the wave will pass through the intermediary layer with only a minor reflection occurring at the interface level. This is beneficial if an active bed is present in the channel.

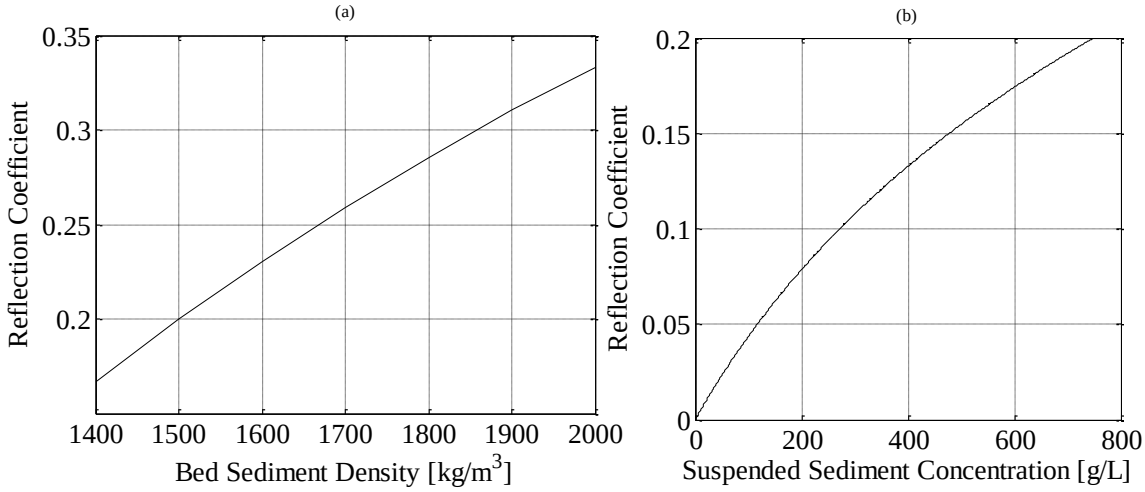

Figure 2.6: Reflection coefficient ratio versus sediment porosity. The reflection coefficient is calculated for density ratios according to the Robins (1990) model, with a water density of 1000 kg/m^3.

2.6 Studies of Factors Affecting TDR

In the field, the salinity, temperature, and the amount of suspended sediment in the channel flow will vary. Each of these parameters has an impact upon the speed of propagation of an EM wave through water. Stogryn (1971) developed several empirical equations that describe the impact of salinity and temperature on the apparent dielectric constant, K_a , which is defined as the square of the ratio of the speed of light in vacuum to the speed of the EM wave in a particular medium. As the TDR device uses a single EM wave, it is possible to use Stogryn's low frequency results for the static dielectric constant, leading to the Equations (2.10) through (2.13). These relations reveal that the apparent dielectric constant is a function of temperature, T and salt concentration, measured in normality units, N . The factors included in Equation (2.10)

are the relationship of the static dielectric constant with temperature only and an empirical equation to account for the concentration of sodium chloride, $a(N)$. The salinity of the salt water, S can be related to the normality, as shown in Equation (2.13).

$$K_a(T,N) = K_a(T,0) \cdot a(N) \tag{2.10}$$

$$K_a(T,0) = 87.74 - 4.008T + 9.398 \cdot 10^{-4} T^2 + 1.410 \cdot 10^{-6} T^3 \tag{2.11}$$

$$a(N) = 1.000 + 0.2551N + 5.151 \cdot 10^{-2} N^2 - 6.889 \cdot 10^{-3} N^3 \tag{2.12}$$

$$N = S\left(1.07 \cdot 10^{-2} + 1.205 \cdot 10^{-5} S + 4.058 \cdot 10^{-9} S^2\right) \tag{2.13}$$

This set of equations can be used to assess the impact of the salinity and temperature upon the TDR measurement. To evaluate these effects, a scenario is constructed in which the salinity varied from 0 PPT to 17.5 PPT, a typical range found in channels near coastal waters (USGS, 2006a; USGS, 2006b). In this analysis, the temperature also varied from 0 to 30 °C. The relative error is computed from an apparent dielectric constant of 80.11, which corresponds to the value at 20 °C and 0 PPT salinity. The results of this analysis are shown in Figure 2.7. As indicated, the impact of salinity and temperature on the dielectric constant is significant (up to 6% relative error).

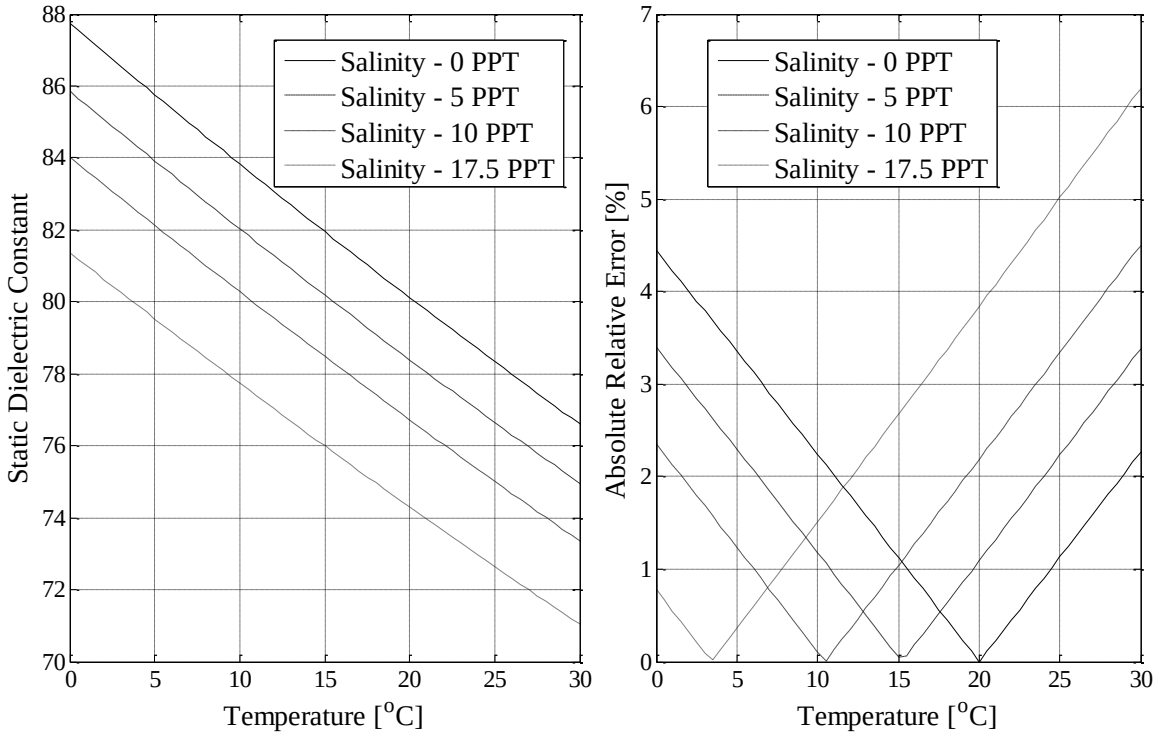

Figure 2.7: Effect of varying channel salinity levels on dielectric constant and TDR measurements. (a) Impact of salinity levels on dielectric constant, per Stogryn (1971). (b) Absolute percentage error in TDR measurements for various temperatures and salinity level

It is also necessary to assess the impact of turbid water with various sediment concentrations upon the performance of a TDR system. Using the method developed by Yu and Yu (2011), it is possible to quantify the changes in the apparent dielectric constant for turbid water. Equations (2.14) and (2.15) are used to calculate the variations in the dielectric constant and relative errors in the resulting TDR measurements. Here, $K_{a,w}$ is the dielectric constant of water, $K_{a,s}$ is the dielectric constant of soil solid, $K_{a,bs}$ is the dielectric constant of saturated sediment, n is the porosity, ρ_{bulk} is the bulk density of the sediment, S is the specific gravity of the sediment and ρ_w is the density of water.

Results are shown in Figure 2.8 (a, b). For typical channel sediment concentrations, the relative error is within 1%.

$$n\sqrt{K_{a,w}}+(1-n)\sqrt{K_{a,s}}=\sqrt{K_{a,bs}} \tag{2.14}$$

$$n=1-\frac{\rho_{\text{bulk}}}{S\times\rho_{\text{w}}} \tag{2.15}$$

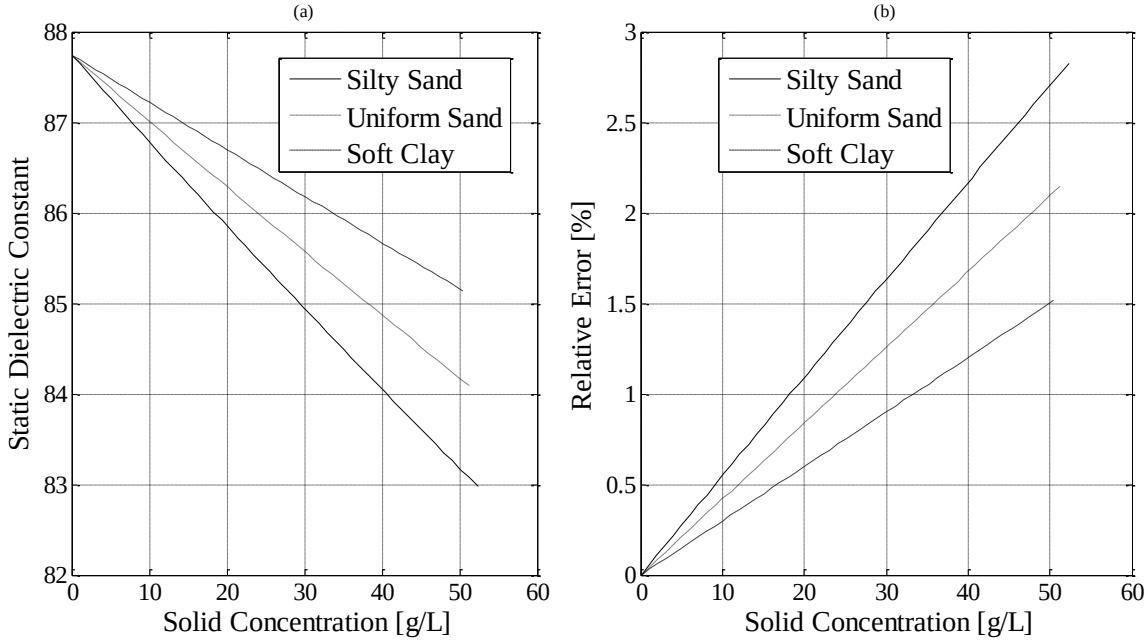

Figure 2.8: Effect of varying channel suspended sediment levels on the dielectric constant and TDR measurements. (a) Impact of sediment levels on dielectric constant for various suspended sediment types, per Yu and Yu (2011). (b) Relative error in TDR measurements versus suspended sediment levels for various sediment types assuming an initial dielectric of pure water. Sediment types as shown in Das (1998).

CHAPTER 3

MEASUREMENT SETUP

3.1 Introduction

To investigate the effects of channel conditions on sonar and TDR instruments, several experiments are conducted in the Clemson Hydraulics Laboratory (CHL). The following section reviews the experimental setup for each of the devices.

3.2 Sonar Experimental Setup

The sonar system consists of an Airmar SS510 transducer, with a sampling frequency of 234 KHz, an 8° beam width, and tolerance of 3 cm, connected to a Campbell Scientific CR-800 data logger. Data is recorded on a work station via the Campbell Scientific PC200 software package. The temperature and salinity tests for sonar are conducted in a 30.5 cm diameter, 1.83 m high test chamber. During the test, the temperature is varied from 5 to 40 °C, measured with a Type K thermocouple for water depths of up to 156 cm. A uniform temperature distribution is maintained by complete mixing of the water. Salinity is varied from 0 to 35.5 PPT, measured with a Vee Gee SX-1 analog refractometer and a DMA 35 Anton Paar density meter. Depths of up to 131 cm are tested for different salinities within this range.

To investigate the effects of turbidity on the sonar device, experiments are conducted in stationary and dynamic configuration, including the effect of stratified turbidity. The static water turbidity tests are conducted in a 183 cm diameter plastic tank with water depths up to 125 cm and turbidity values from 39 to 520 NTU. The dynamic

turbidity tests are conducted in the CHL flume with a depth of 56 cm, for flow velocity ranging from 4 to 12 cm/s. The stratified turbidity flow tests are also conducted in the same flume for depths from 55 to 61 cm, velocity from 5.5 to 12 cm/s, and a stratified turbidity layer of 7 to 17 NTU in the main flow and 300 to 900 NTU in the bottom 5 cm, as shown in Figure 3.1. For each of these tests, the turbidity is measured with a Global Water WQ 730 turbidity sensor connected to the GL 500U data logger.

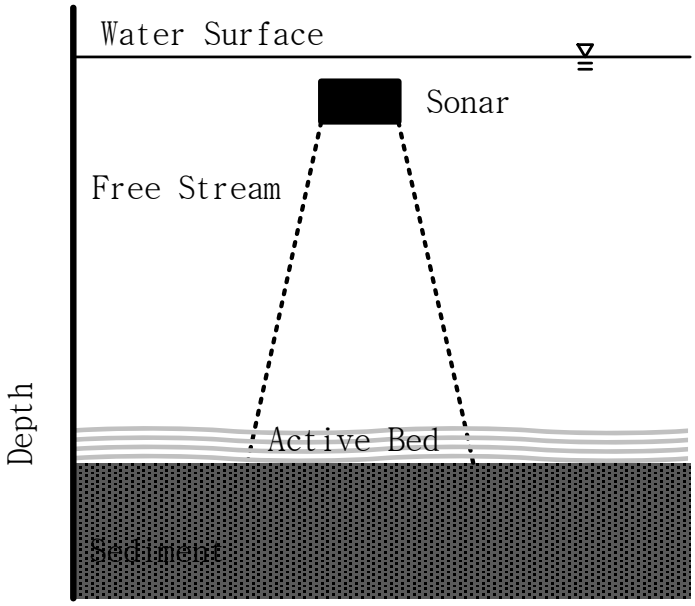

Figure 3.1: Schematic setup for the turbidity stratification test.

In addition to temperature, salinity, and turbidity effects on sonar, the effect of the bed contour is also investigated. Two series of tests are conducted with cones of 15 and 23 cm in diameter, which are placed underneath the sonar. To create a planar reflecting surface, the cone is partially filled with sand as shown in Figure 3.2.

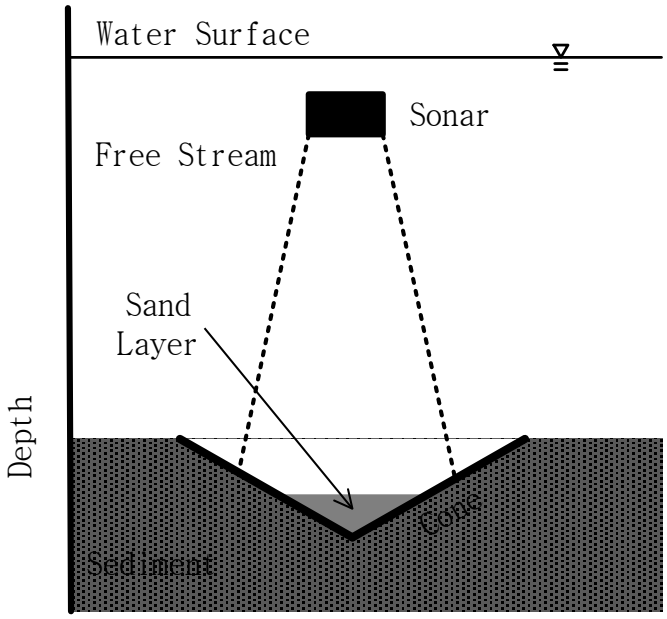

Figure 3.2: Schematic setup for the scour hole/beam ratio tests.

3.3 TDR Experimental Setup

The TDR system used to investigate the effects of temperature, salinity, and turbidity on measurements consists of a probe similar to that used by Yankielun and Zabilansky (1999), as shown in Figure 3.3. The waveform is generated by the TDR 100, from Campbell Scientific, and is recorded on a work station running the Campbell Scientific PC TDR software. The tests are conducted in a 60 cm diameter barrel, with the lower portion of the TDR probe located in sand with an AFS grain fineness number of 16 and the upper portion completely submerged in the water, as shown in Figure 3.3. The temperature tests are conducted at two water depths, 73.5 and 58.5 cm, with temperatures from 7 to 40 °C. During the salinity tests, the concentration varied from 0 to 0.75 PPT, in 0.25 PPT increments, for a water depth of 69 cm. The effect of turbidity on the TDR

readings is evaluated by introducing water depth of 52.5 cm with sediment concentration ranging from 100 NTU to 500 NTU.

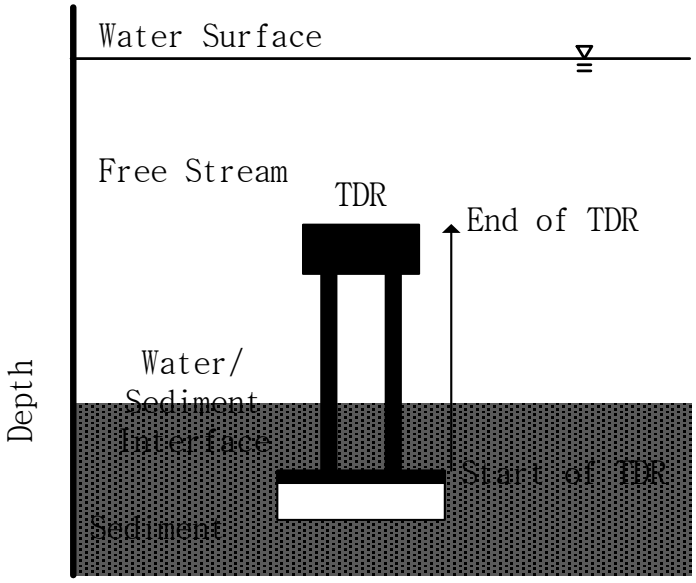

Figure 3.3: Schematic of the TDR setup.

CHAPTER 4

RESULTS FROM SONAR TESTS

4.1 Introduction

Experimental results from sonar tests are presented in this chapter. Tests were conducted by varying temperature, salinity, turbidity, and bed topography.

4.2 Temperature Effects

The temperature tests on the sonar device are conducted at depths of 94.5, 125, and 156 cm. The tests revealed that the percent relative error, relative to the 20 °C sonar reading, diverge from zero as the temperature deviates from the reference. For the three depths (94.5, 125, and 156 cm), the percent relative errors in the sonar readings range from -3.30% to 3.30%, -4.97% to 1.77% and -5.98% to 2.00%, respectively, as shown in Figure 4.1, Figure 4.2 and Figure 4.3. There is no specific trend for the three depths except that the variation range increases with increase in water depth.

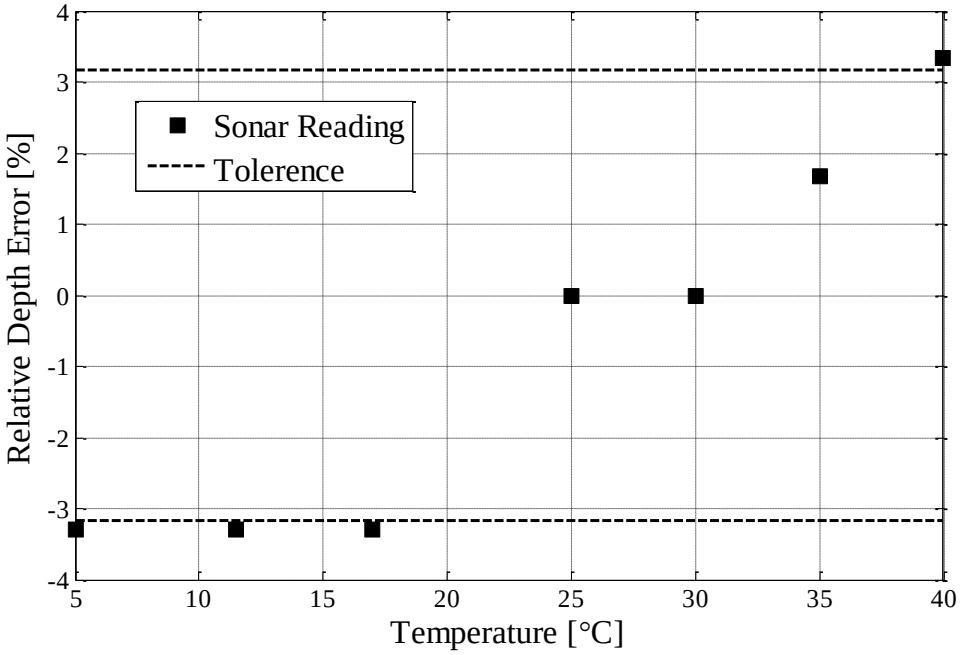

Figure 4.1: Variation in relative error of sonar measurements with temperature for water depth of 94.5 cm.

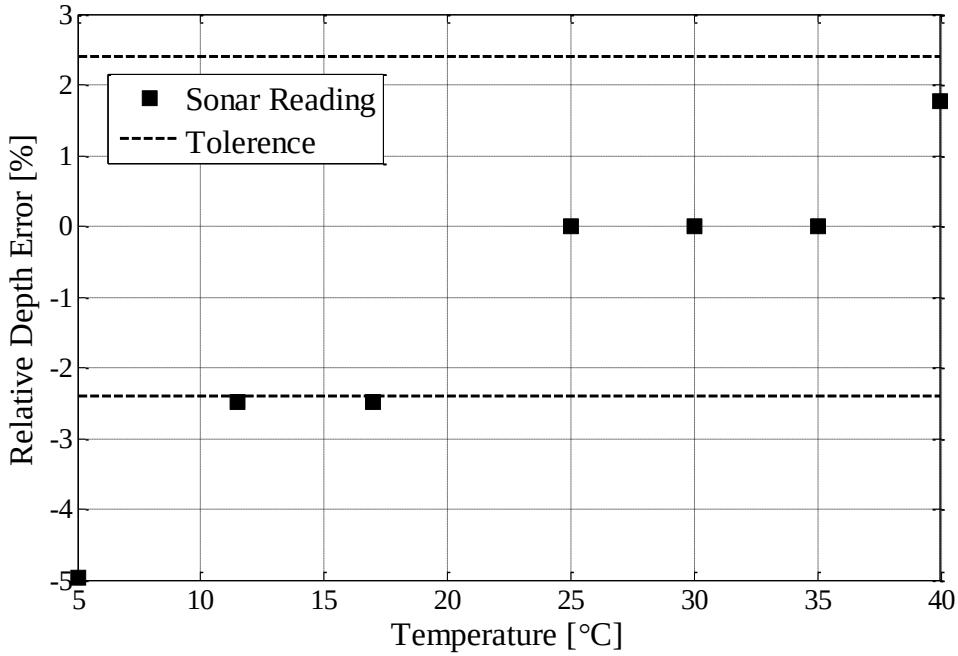

Figure 4.2: Variation in relative error of sonar measurements with temperature for a water depth of 125 cm

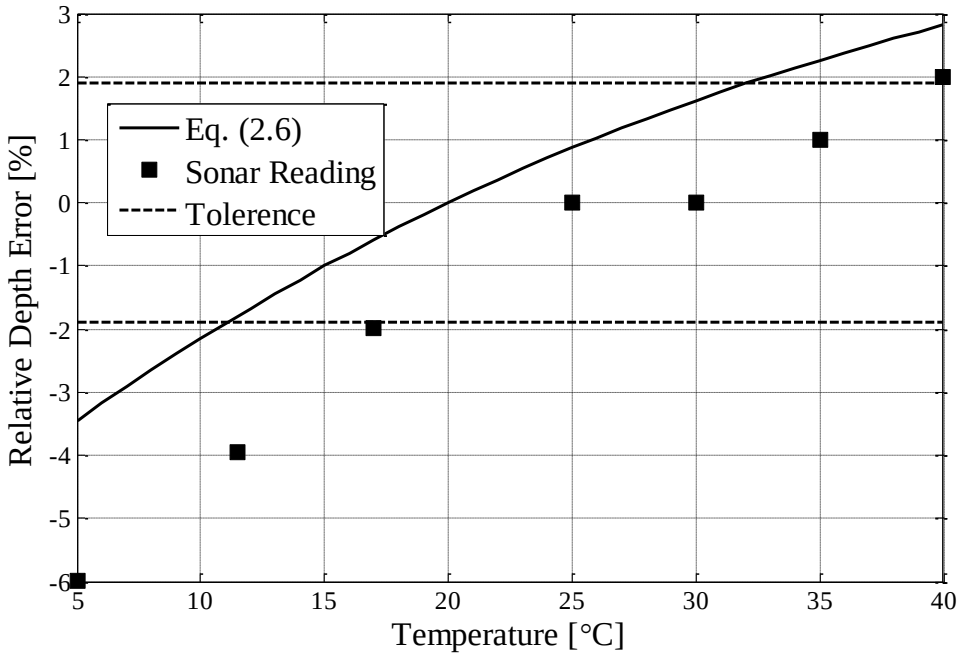

Figure 4.3: Variation in relative error of sonar measurements with temperature for a water depth of 156 cm.

This result suggests that as the channel temperature changes seasonally, the distance to the bed, and any scour depth will artificially vary, simply due to changes in the flow temperature. The experimental results follow the same trend as the Mackenzie model predictions (Figure 2.3). The deviation between the two results may be accounted for by the precision of the sonar transducer ($\pm$ 3 cm).

Therefore, to account for temperature changes, the temperature around the sonar transducer should be measured along with the sonar signal. It must be noted that as the depth of the channel increases, the sonar readings are affected to a greater degree by the temperature since the error is proportional to the distance traveled by the acoustic pulse.

4.3 Salinity Effects

The salinity tests on sonar are conducted for two water depths (116 and 131 cm). The results obtained from the test, as shown in Table 4.1, range from 3.51 to 3.81% relative error (relative to zero salinity). These values are in line with the errors predicted in CHAPTER 2 with the Mackenzie model. The model reveals that for the same range of salinity, the error could reach up to 3.18 %.

Table 4.1: Range of percent relative error in water depth, and comparison with theoretical model.

Water depth, [cm]	Range of salinity, [PPT]	Measured relative error in water depth, [%]	Relative error (from Mackenzie model,1981), [%]
116	0 to 35.5	0 to 3.51	0 to 3.18
131	0 to 35.5	0 to 3.81	0 to 3.18

The results in Table 4.1 suggest that if the sonar transducer is located within 131 cm of the bed, the influence of salinity on the measurements is likely to be minor. This presents a tradeoff, however, between the ease of maintenance in the field, which is complicated by installations close to the bed, and measurement error.

4.4 Turbidity Effects

Turbid waters are commonly encountered in natural rivers. To evaluate the impact of the suspended particles on the sonar readings, three cases are considered. In the first case, the sonar is tested in still turbid water in a tank; in the second case, the sonar is tested in

flowing turbid water in a flume; lastly, the effect of turbidity stratification on sonar accuracy is evaluated. For the still turbidity test, the water depth is varied from 94.5 to 128 cm and the concentration is varied from 39 to 525 NTU. Table 4.2 shows the results. It indicates that the still turbidity has a negligible effect on the sonar's bed measurements.

Table 4.2: Range of percent relative error in water depth for various turbidities

Water depth, [cm]	Range of relative error in water depth, [%]	Tolerance limit, [%]	Range of turbidity, [NTU]
94.5	0 to 3.3	-3.2 to 3.2	39 to 525
113	0 to 2.8	-2.73 to 2.73	39 to 525
128	0 to 0	-2.4 to 2.4	39 to 525

The combined effects of suspended particles and channel flow are evaluated in a flume for a water depth of 56 cm, the results of which are shown in Figure 4.4 and Figure 4.5. In Figure 4.4, the relative percent errors for a 30 second sample mean are plotted for various average velocities and turbidity levels in the channel. Figure 4.4 shows that as the velocity increases, for all turbidities tested, the absolute relative error increases. Additionally, it appears that the level of turbidity has little effect on the measured error. For example, for a turbidity of 402 NTU, the relative error varies from -6.12 to 0.41%, while for 220 NTU the relative error varies from -6.82 to -2.1%. Figure 4.4 reveals that the increase in turbidity does not lead to an increase in relative error.

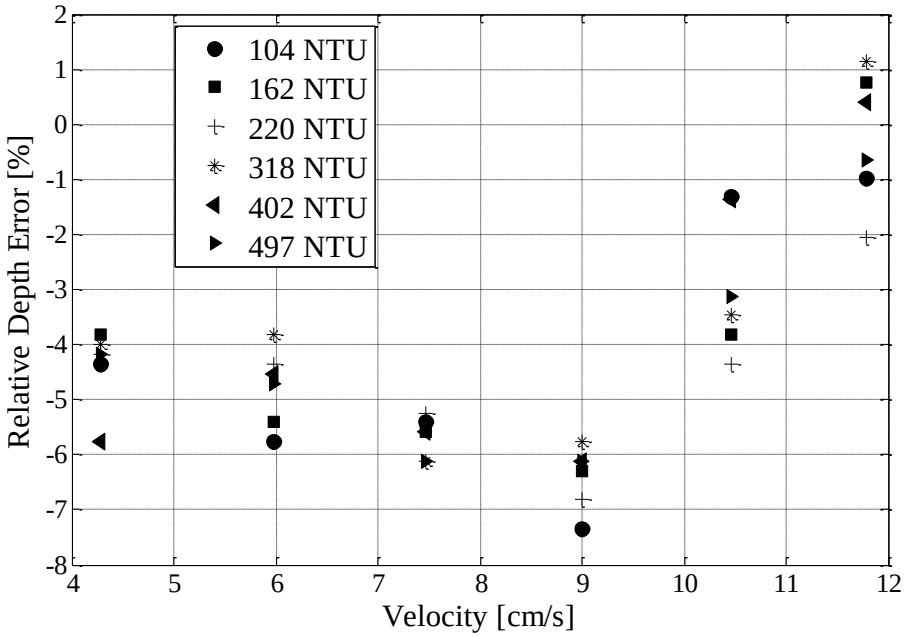

Figure 4.4: Relative Error in the sonar reading for various turbidity concentrations and velocities of the channel flow.

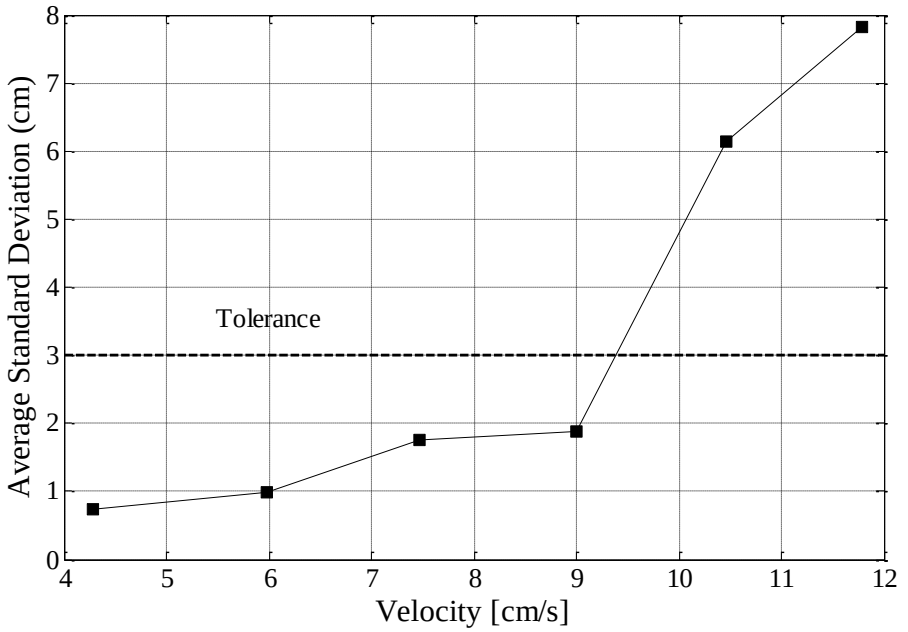

Figure 4.5: Average standard deviation of sonar readings from Figure 4.4.

In Figure 4.4, it should be noted that for velocities greater than 9 cm/s, there is a step change in the relative percent error. The source of this divergence is revealed in Figure 4.5, where for these same higher velocities, the standard deviation in the 30 second time histories increases sharply to a level above the sonar device tolerance. This indicates that for the two highest velocities, the sonar device is not able to locate the bed. Thus, the combined results in Figure 4.4 and Figure 4.5 reveal that as the velocity of a turbid flow increases beyond 9 cm/s, the sonar can no longer obtain a stable recording. The inability to locate the bed is attributed to an increase in the scattering by the particles in the channel due to an increase in the apparent concentration of suspended solids moving beneath the sonar transducer due to the higher flow velocity.

The results in Figure 4.4 and Figure 4.5 indicate that when the standard deviation of the sonar time history exceeds the device tolerance, the average value from sonar time history is inaccurate and scour readings should be independently verified with another device. Also, the results suggest that for sites with higher sediment loads during peak flow conditions, another device should be deployed instead of sonar.

In the final turbidity test configuration, the effect of a stratified concentration, layer thickness, and flow velocity are considered. The velocity ranges from 4 to 12 cm/s, the stratified layer thickness varies from 2 to 5 cm, and the concentration in the stratified layer is between 300 and 900 NTU. The flow depths during the tests range from 55 to 61 cm. The results of these experiments reveal that for low velocities, and layers of increasing thickness in the depth dimension, the relative error can be as high as 17.5%.

For stratified layers of smaller thickness in the depth dimension, this error drops down to 2%, which is of the order of the dimension of the layer.

As it was with the uniform turbidity test, it is also important to investigate the standard deviation of the measured signal. As evident in Figure 4.6, the standard deviation of the 30 second time histories is above the sonar device tolerance limit for all concentrations. This indicates that the sonar device is unable to determine the bed level. This result disagrees with Robbins (1990) model suggesting that the stratification effects are not well described by considering density alone. Therefore, other effects, such as increased scattering or attenuation by the sediment particles, must also be considered.

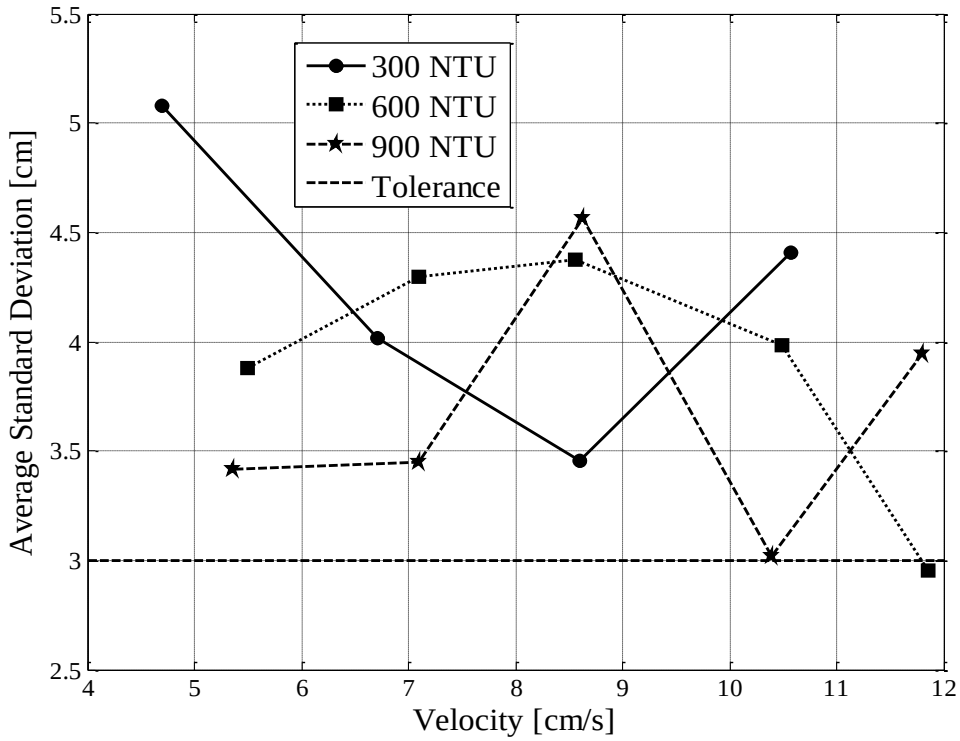

Figure 4.6: Standard deviation of sonar for stratification concentration and velocity ranges.

In summary, sonar is affected by moving turbid water. For a uniform turbidity, and for velocities higher than 9 cm/s (for turbidity concentration ranging from 100 to 500 NTU) the sonar device cannot determine the bed level. For stratified flow, this affect occurs even for low velocities. As such, the findings suggest that sonar devices should not be used independently in highly turbid zones. It is important to monitor the standard deviation of the recorded signal to confirm that the sonar readings are reliable.

4.5 Topography and Beam Width Effect

Naturally developed scour holes have uneven surfaces. Therefore, it is important to determine the location in the bed topography that is registered by sonar pulse. Two cases were considered here, one in which the sonar beam falls entirely within the scour hole, Case A in Figure 4.7, and the other one in which the sonar beam completely surrounds the scour hole, Case B. In Case A, the sonar beam reflects along the surfaces from point Q (the minimum depth) to point R (the maximum water depth). In Case B, however, the minimum depth corresponds to the unscoured bed level, located by point P. These two conditions are reproduced in the lab. The results are shown in Table 4.3 and Table 4.4.

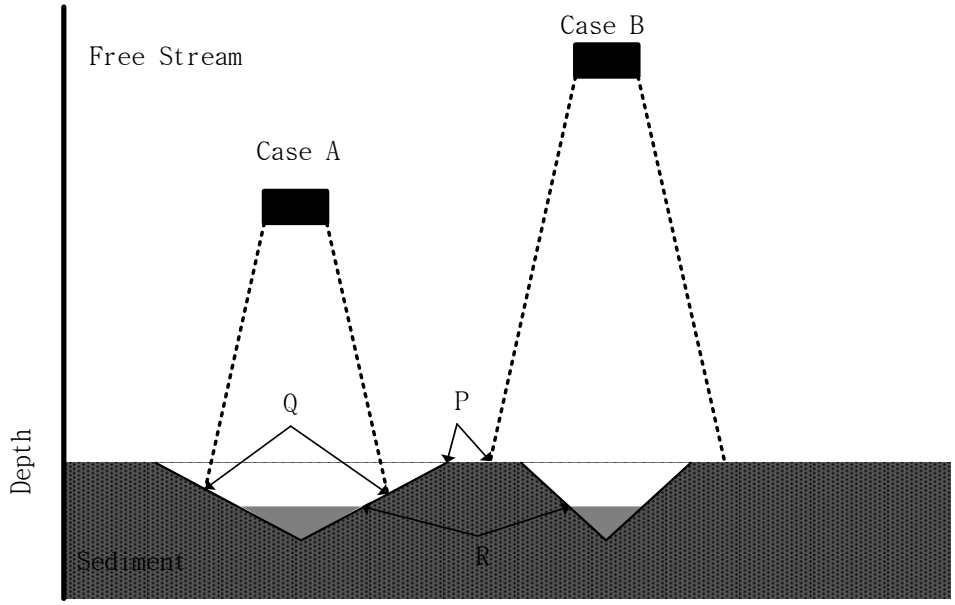

Figure 4.7: Sonar beam to scour hole size experimental setup.

Table 4.3: Experimental results for Case: A

Maximum Water Depth, R [cm]	Minimum Water Depth, Q [cm]	Average of R and Q [cm]	Actual Sonar Reading [cm]
85.3	76.7	81.0	76.2 ± 3
75.9	68.25	72.1	67 ± 3
63.7	57.2	60.45	54.9± 3

Table 4.4: Experimental results for Case: B

Maximum Water Depth , R [cm]	Minimum Water Depth, P [cm]	Actual Sonar Reading [cm]
111.56	103.63	100.6 ± 3
84.43	77.11	79.3 ± 3
74.68	67.06	64.0 ± 3
54.25	46.94	48.8 ± 3
45.72	38.40	39.6 ± 3

According to Table 4.3, the measured sonar readings are within the device tolerance limit of point Q for Case A. Similarly, for Case B, Table 4.4 indicates that the measured sonar results correspond to point P. From these two results, it can be concluded that the sonar measurements correspond to the minimum depth encountered by the beam, which does not correspond to the point of maximum scour. Therefore, in the field if the beam is contained within the hole, sonar is expected to underestimate the scour depth. Alternatively, if the sonar transducer is located far from the bed, due to installation or maintenance concerns, and if the beam diameter is larger than the scour hole, the presence of scour cannot be identified.

CHAPTER 5

RESULTS FROM TDR TESTS

5.1 Introduction

The performance of the TDR system in varying channel salinity, temperature, and turbidity are discussed in the following sections.

5.2 Temperature Effects

As discussed previously, the dielectric constant is a function of temperature and decreases with increasing water temperature (Stogryn, 1971). Results for the TDR probe under various water temperatures are shown in Figure 5.1. The curves in Figure 5.1 are the reflected waveforms analyzed using the method outlined by Yankeilun and Zabilansky (1999). Near the start of the waveform, a sharp reflection occurs indicating the start of the probe. This is then followed by a 'plateau A' at a reflection coefficient of -0.2, corresponding to the depth of sediment. This plateau then decreases in a step to 'plateau B' with a reflection coefficient of approximately -0.4, indicating the presence of water. Finally, at the end of the probe there is a terminal step change. Figure 5.1 therefore indicates that as the temperature increases, the waveform shifts such that it gives a decreasing trend of apparent length.

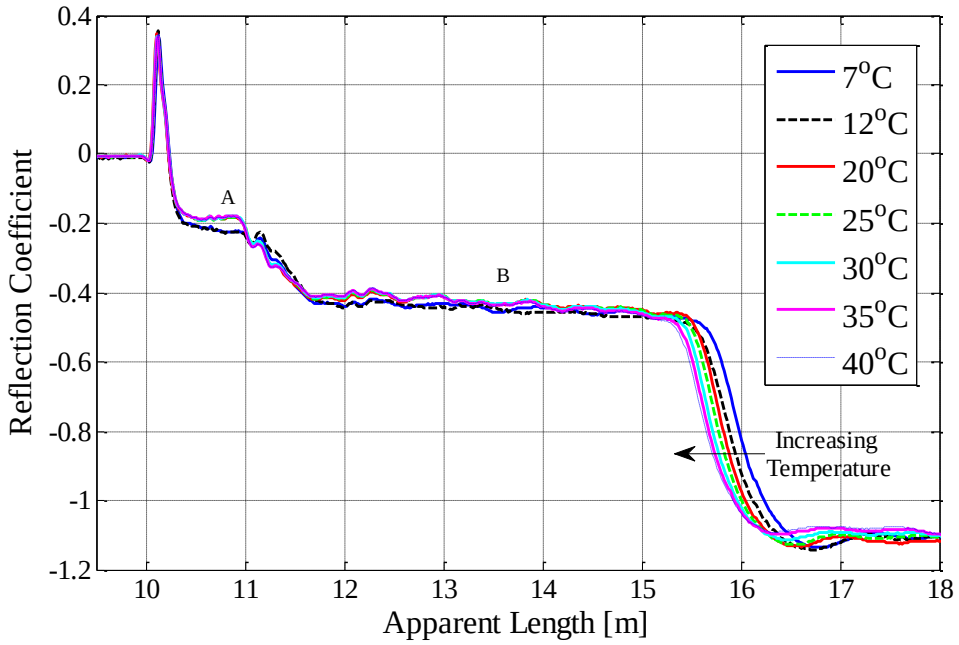

Figure 5.1: TDR waveform in various water temperatures for a depth 58.5 cm.

Temperature tests on TDR system are performed for two water depths (73.5 cm and 58.5 cm). Water depths extracted from TDR waveform are then converted to percent relative error, relative to the dielectric constant at 20 °C. Figure 5.2 and Figure 5.3 show the percent relative errors in the measured results, for the water depth of 73.5 and 58.5 cm, respectively, along with the predictions from Stogryn (1971) model.

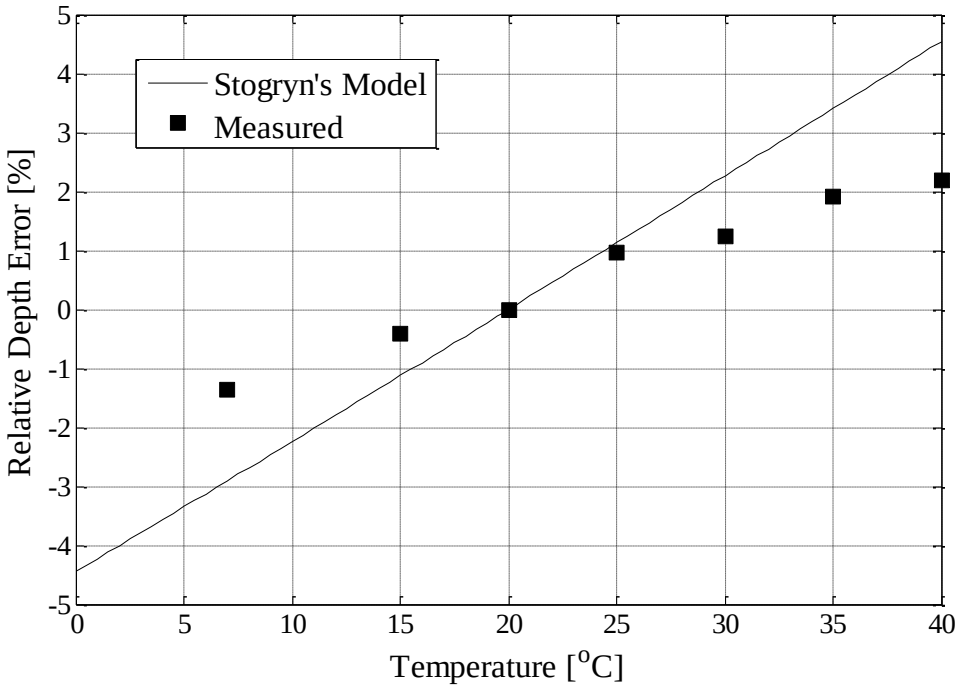

Figure 5.2: Relative error in the TDR reading for various temperatures and a water depth of 73.5 cm.

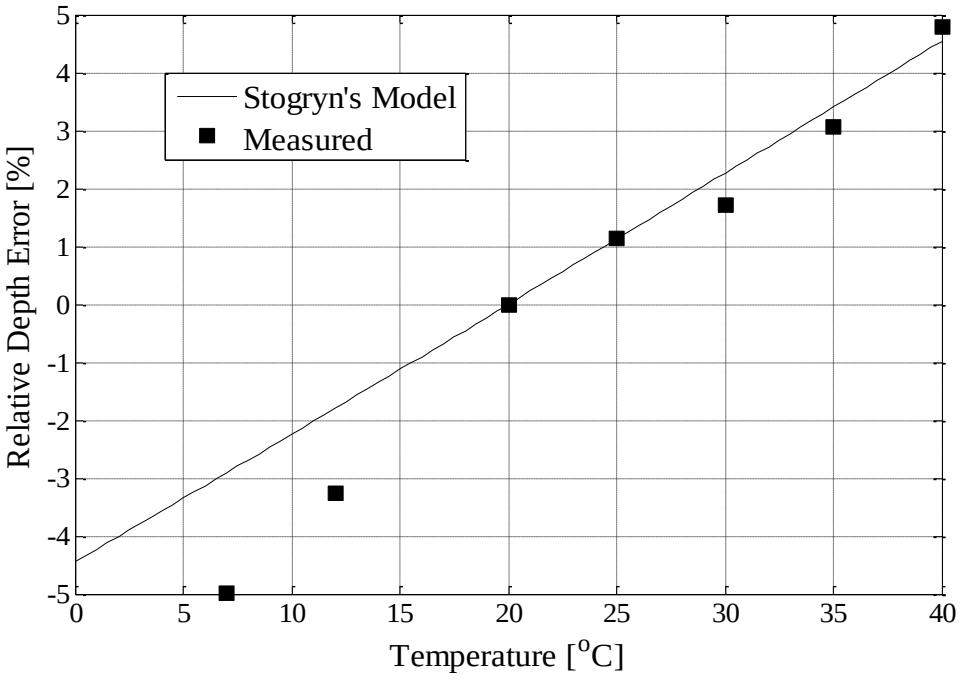

Figure 5.3: Relative error in the TDR reading for various temperatures and a water depth of 58.5 cm.

In general, the figures indicate that lower water depths are measured by the TDR as temperature increases above 20 °C and that higher depths are measured as the temperature decreases below 20 °C. The percent relative error in water depth ranged from -1.36% to 2.18% and -4.98% to 4.78% for 73.5 cm and 58.5 cm of water depth, respectively. As shown in Figure 5.2 and Figure 5.3, the measured values determined by the TDR method are affected by a change in the water temperature. Practically, this suggests that in the winter season, the TDR might overestimate the scour depth while in summer TDR might underestimate the scour depth. The temperature dependency of the measurements can be accounted for by measuring temperature as part of the scour monitoring system.

5.3 Salinity Effects

The salinity of the flow can also affect the accuracy of a TDR system as indicated by Stogryn (1971). Thus, TDR is tested under various salinity conditions, for which the resulting waveforms are shown in Figure 5.4.

The TDR waveform, particularly the reflection at the end of the probe, becomes increasingly hard to distinguish as the salinity increases. Above 0.5 PPT, the reflection at the end of the probe is indistinguishable. This degradation in performance can be attributed to the decay of the EM wave into the surrounding medium, which becomes more conductive as the salinity increases.

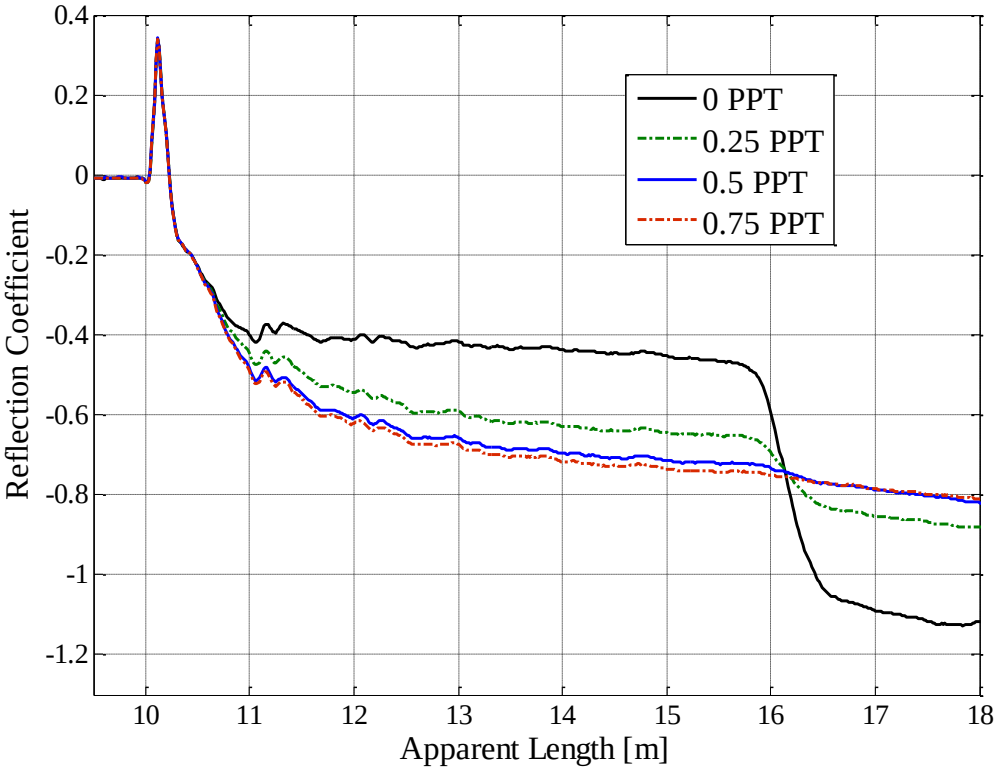

Figure 5.4: Sensitivity of TDR waveform to salinity.

Therefore, deploying a TDR device in a saline environment or at sites that could become brackish (greater than 0.5 PPT) can lead to inconclusive results, due to the loss in the distinct features of the waveform necessary to determine the scour depth.

5.4 Turbidity Effects

The results obtained for the turbidity tests conducted on the TDR system for a water depth of 52 cm are shown in Figure 5.5. The effect of turbidity on TDR measurements are determined by calculating the percent relative error in water depths. For turbidities up to 500 NTU, the TDR system is insensitive to the presence of

suspended sediments. The results shown in Figure 5.5 imply that the TDR system can be efficiently operated in highly turbid zones (maximum error up to 5%).

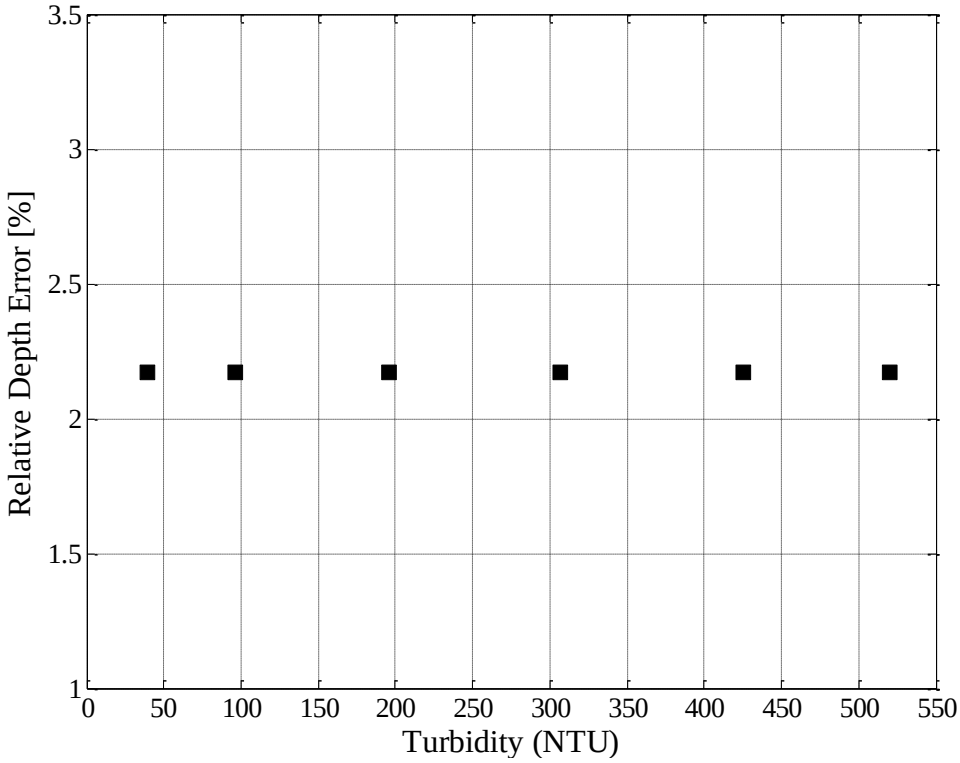

Figure 5.5: Effect of turbidity on TDR

CHAPTER 6

CONCLUSIONS

6.1 Summary of the research

Channel conditions changes with time in terms of temperature, salinity, turbidity, and bed topography in natural channels. These changes can have substantial effects on real time scour monitoring systems. An extensive experimental campaign is conducted to evaluate two common scour measurement devices: sonar transducer and time-domain reflectometry probe.

For the sonar device, changes in the temperature can result in relative errors up to 6% in channel depth. The temperature dependency can be accounted for in the field by measuring the temperature and accounting for the change in the speed of sound. Salinity can lead to relative errors of up to 3%, which can also be accounted for by correcting the scour measurements according to the measured salinity levels. The concentration of suspended particles minimally affects the sonar results in still water. For dynamic turbidity, uniform as well as stratified, the relative error in bed level measurements can be significant. The results indicate that measuring the standard deviation of the recorded signal is important to ascertain the validity of the averaged result obtained from the sonar measurements. Lastly, for variable bed topography, the sonar measures the shallowest depth. Therefore, the beam width at the bed with respect to scour hole may significantly affect the accuracy of the scour depth measurements.

For the TDR device, the channel temperature can have a significant effect on the measured depth of a scour hole. The relative errors can be of the order of 5%. This effect, however, can be mitigated by monitoring the channel temperature in addition to the TDR waveform. Salinities greater than 0.5 PPT result in a loss of the distinct features in the TDR waveform necessary to determine scour depth. It is recommended to only install the TDR in freshwater conditions. Turbidity in the channel flow had no measurable effect on the TDR measurements and thus the TDR can be used for monitoring scour in highly turbid zones.

6.2 Outcome

The work presented in this manuscript has detailed operational sensitivities of two scour monitoring devices by considering the physical principles behind the operation of each device. Additionally, through a series of detailed experiments, these sensitivities have been evaluated in order to assess the impact on scour measurements. Based upon the results presented, it is possible to evaluate potential scour monitoring sites and to select methods that are insensitive to the anticipated channel conditions, resulting in more robust field measurements.

BIBLIOGRAPHY

Arneson, L.A., Zevenbergen, L.W., Lagasse, P.F., Clopper, P.E., (2012). "Hydraulic Engineering Circular No.18: Evaluating Scour at Bridges, 5th Ed.", U.S. Dept. of Transportation, Federal Highway Administration, Publication No. FHWA-HIF-12-003.

Butch, G.K., (1996). "Evaluation of Selected Instruments for Monitoring Scour At Bridges in New York.", North American Water and Environment Congress, ASCE.

Brice, J. C., and Blodgett, J. C. (1978). "Countermeasures for Hydraulic Problems at Bridges," Vol. 1 & 2, FHWA/RD-78-162 & 163, Federal Highway Administration, U.S. Department of Transportation, Washington, D.C.

Cooper, T., Chen, H. L., Lyn, D., Rao, A. R., Altschaeffel, A.G., (2000). " A Field Study of Scour-Monitoring Devices for Indiana Streams: Final Report" FHWA/IN/JTRP-2000/13, October 2000.

Das, B. M., (1998). Principles of Geotechnical Engineering, 4th Ed., PWS Publishing Company, Boston, Ma.

DeFalco, F., Mele, R., (2002). "The Monitoring of Bridges for Scour and Sedimentri", *NDT&E International*, Vol. 35, pp. 117-123.

Deng, L., Cai, C.S., (2010). "Bridge Scour: Prediction, Modeling, Monitoring, and Countermeasures—Review". *Practice Periodical on Structural Design and Construction*, Vol. 15, Issue 2, pp. 125-134.

Ettema, R., Zabilansky, L., (2004). "Ice Influences on Channel Stability: Insights from Missouri's Fort Peck Reach", Journal of Hydraulic Engineering, Vol. 130, No. 4, A.S.C.E, pp. 279-292.

Fisher, M. (2012). "Analysis and Evaluation of Existing and Novel Turbulent Dynamic Pressure Based Methods for Measuring Bridge Pier and Abutment Scour". Ph.D. Thesis. Clemson University, USA.

Gray, J. R., Melis, T. S., Patiño, E., Larsen, M. C., Topping, D. J., Rasmussen, P. P., Figueroa-Alamo, C. (2003, October). US Geological Survey research on surrogate measurements for suspended sediment. In Proceedings of the 1st Interagency Conference on Research in Watersheds (pp. 95-100).

Bibliography (continued)

Guo, N., Cawley, P., Hitchins, D., (1992). The finite element analysis of the vibrational characteristics of a piezoelectric disks. *Journal of Sound and Vibration*, 159(1), 115-138.

Hamilton, E. L., (1980). "Geoacoustical Modeling of the Sea Floor", *Journal of the Acoustical Society of America*, Vol. 68, No. 5, pp. 1313-1340.

Holnbeck, S. R., McCarthy, P. M., (2011). "Monitoring Hydraulic Conditions and Scour at I-90 Bridges on Blackfoot River Following Removal of Milltown Dam Near Bonner, Montana, 2009" in *Scour and Erosion: Proceedings of 5th International Conference on Scour and Erosion.* Ed: Burns, S.E., Bhatia, S.K., Avila, C. M. C., Hunt, B. E., November 7-10, 2010, San Francisco, CA., A.S.C.E.

Hunt, B. E., (2005). "Scour Monitoring Programs for Bridge Health." *Transportation Research Record: Journal of the Transportation Research Board*, Washington D.C., pp.: 531-536.

Hunt, D. (2009). "Monitoring Scour Critical Bridges." NCHRP Synthesis 396, Transportation Research Board, Washington, DC.

Jaffe, H., Berlincourt, D.A., (1965). "Piezoelectric transducer materials". Proceedings of the IEEE, 53(10), 1372-1386.

Kuwahara, S., (1939), "Velocity of Sound in Sea Water and Calculations of the Velocity for Use in Sonic Soundings". *Hydrogeologic. Review*., v. 16, p. 123-140.

Leroy, C.C., (1969). "Development of Simple Equations for Accurate and More Realistic Calcualtion of the Speed of Sound in Seawater*", The Journal of the Acoustical Society of America*. Vol. 46, No. 1B.

Lagasse, P. F., E. V. Richardson, J. D. Schall, and G. R. Price (1997). "Instrumentation for Measuring Scour at Bridge Piers and Abutments". NCHRP Report 396: TRB, National Research Council, Washington, D.C.

Lin, Y. B., Lai, J. S., Chang, K. C., Li, L. S., (2006). "Flood Scour Monitoring System Using Fiber Bragg Grating Sensors" *Smart Materials and Structures*, Vol. 15, pp. 1950-1959.

MacKenzie, K.V., (1981). "Nine-term Equation for Sound Speed in the Oceans" *Journal of the. Acoustical. Society of. America*, Vol.70, Issue 3, pp. 807-812.

Bibliography (continued)

Mason, R. R., Sheppard, D. M., (1994). "Field Performance of an Acoustical Scour-Depth Monitoring System". In Fundamentals and Advancements in Hydraulic Measurements and Experiments, Ed: Pugh, C.A., Proceedings of the Symposium, Buffalo, N.Y., August 1-5, 1994. A.S.C.E.

Mueller, D. S. (2000). "National Bridge Scour Program-Measuring Scour of the Streambed at Highway Bridges." U.S. Geological Survey, Reston, Va.

Murillo, J.A., (1987). "The Scourge of Scour", Civil Engineering, July 1987, A.S.C.E., pp: 66-69.

Nassif, H., Ertekin, A. O., Davis, J., (2002). "Evaluation of Bridge Scour Monitoring Methods: Final Report" Federal Highway Administration, Report FHWA-NJ-2003-09, March, 2002.

N.T.S.B., (1987). "Collapse of New York Thruway (I-90) Bridge, Schoharie Creek, Near Amsterdam, New York, April 5, 1987", NTSB Number: HAR-88/02, NTIS Number: PB88-916202.

N.T.S.B., (1989). "Collapse of The Northbound U.S. Route 51 Bridge Spans Over The Hatchie River, Near Covington, Tennessee, April 1, 1989", NTSB Number: HAR-90/01, NTIS Number: PB90-916201.

Parker, G. W., Bratton, L., and Armstrong, D. S. (1997). "Stream Stability and Scour Assessments at Bridges in Massachusetts." U.S. Geological Survey Open File Report No. 97-588 (CD-ROM), Massachusetts Highway Dept. Bridge Section, Marlborough, Mass., 53.

Rhodes, J., Trent, R., (1993). "Economics of Floods, Scour and Bridge Failures" in Hydraulic Engineering '93: Proceedings of 1993 Conference. Ed: Shen, H.W., Su, S. T., Wen. F., July 25-30, 1993, San Francisco, CA, A.S.C.E.

Richardson, J.R., Price, J., (1993). "Emergent Techniques in Scour Monitoring Devices" in Hydraulic Engineering '93: Proceedings of 1993 Conference. Ed: Shen, H.W., Su, S. T., Wen. F., July 25-30, 1993, San Francisco, CA, A.S.C.E.

Robins, A. J. (1990). "Reflection of Plane Acoustic Waves From a Layer of Varying Density." *Journal of the Acoustical Society of America*, Vol. 87, No 4, pp. 1546-1552.

Stogryn, A., (1971). "Equations for Calculating the Dielectric Constant of Saline Water", *IEEE Transactions on Microwave Theory and Techniques*, August, 1971, pp. 733-736

Bibliography (continued)

Stoll, R. D., Kan, T. K., (1981). "Reflection of Acoustic Waves at a Water-Sediment Interface", *Journal of the Acoustical Society of America*, Vol. 70, No. 1, pp. 149-156.

Urick, R. J., (1975). Principles of Underwater Sound, McGraw-Hill Inc, New York, USA.

USGS, (2006a), "Water Data Report 2006: 02172053 Cooper River at Mobay Near North Charleston, S.C.", U.S. Dept. of Interior, U.S. Geological Survey.

USGS, (2006b), "Water Data Report 2006: 02156500 Broad River Near Carlisle, S.C.", U.S. Dept. of Interior, U.S. Geological Survey.

Yankielun, N.E., Zabilansky, L. (1999). "Laboratory Investigation of Time Domain Reflectometry System for Monitoring Bridge Scour", *ASCE Journal of Hydraulic Engineering*, Vol. 125, No. 12 pp. 1279-1284.

Yu, X., Yu, X., (2006). "Time Domain Reflectometry Tests of Multilayered Soils" Proceedings of the TDR 2006, Purdue University, West Lafayette, U.S.A., Sept. 2006.

Yu, X., Yu, X., (2011). "Development and Evaluation of an Automatic Algorithm for a Time-Domain Reflectometry Bridge Scour Monitoring System" *Canadian Geotechnical Journal*, Vol. 48 pp. 26-35.

Yu, X., Zabilansky, L. J., (2006). "Time Domain Reflectometry for Automatic Bridge Scour Monitoring", in GeoShanghai 2006: Site and Geomaterial Characterization, GSP 149. Ed. Puppala, A. J., Fratta, D., Alshibli, K., and Pamukcu S., A.S.C.E.

Zabilansky, L., Ettema, R., Weubeen, J., Yankielun, N., (2002). "Survey of River Ice Influences on Channel Bathymetry Along the Fort Peck Reach of the Missouri River, Winter 1998–1999", Technical Report ERDC/CRREL TR-02-14., US Army Corps of Engineers, Engineer Research and Development Center, September, 2002.